

SUPPLEMENTARY INFORMATION

Ultrafast photoelectron spectroscopy of photoexcited aqueous ferrioxalate

L. Longetti,[†] T.R. Barillot,[†] M. Puppini,[†] J. Ojeda,[†] L. Poletto,[‡] F. van Mourik,[†]
C.A. Arrell,^{†,¶} and M. Chergui^{*,†}

[†]*Laboratory of Ultrafast Spectroscopy and the Lausanne Centre for Ultrafast Science, ISIC,
Ecole Polytechnique Fédérale de Lausanne, CH-1015 Lausanne, Switzerland*

[‡]*National Research Council of Italy - Institute of Photonics and Nanotechnologies
(CNR-IFN), via Trasea 7, 35131 Padova, Italy*

[¶]*now at: Laboratory for Advanced Photonics, Paul Scherrer Institut, CH-5232 Villigen,
Switzerland*

E-mail: majed.chergui@epfl.ch

S1 Laser-assisted photoelectric effect (LAPE) on pure solvent

The LAPE effect consists in the appearance of replicas of the PE spectrum when pump and probe pulses simultaneously impinge on the sample. This has been previously described for time-resolved photoemission on liquids¹. The LAPE signal is present in each tr-PES spectra at $t=0$ when the pump and probe pulses overlap. An example is given in Figure S1.a as the intense (red) signal around time zero. This is the first-order replica at 6.5 eV of the water HOMO peak ($E_B=11.16$ eV and 4.7 eV pump-pulse field) that occurs within the RoI. It is more intense than the photoexcited solute signal, which actually starts at time zero and

remains. A LAPE characterisation is needed to deconvolve it from the rising signal.

Because LAPE is observed in any sample, we performed a tr-LPES measurement on pure solvent (water) in the very same experimental conditions. The result is shown in Figure S1.c, where no overlap with any other signal occurs. The LAPE width in time corresponds to the cross-correlation of pump and probe pulses¹, therefore it is symmetric for gaussian pulses and is exploited to characterise the instrumental response function (IRF) of the current experiments.

The fit of a gaussian curve (red trace) has a FWHM of (96 ± 4) fs. This value was used to deconvolve the IRF from the real signal dynamics in the fitting of the kinetic traces and to therefore isolate the transient PE rise time of the photoexcited molecules.

S2 Photoelectron spectrum feature assignment

The assignment of the PES feature of ferrioxalate ground state and upon photoexcitation with 263 nm pulses, both shown in the manuscript and here reported, respectively, in Figure S2.a and S2.b, is accomplished by referring to the PE spectra of iron compounds in aqueous solution reported by Seidel *et al.*², also shown in Figure S2.c. Here the PE spectra are from hexa-aquated iron compounds in water with different oxidation states: the upper spectrum is a ferrous species (Fe^{2+}) and the lower spectrum corresponds to ferric species (Fe^{3+}). Beside the different coordinated ligands (water in the reference, oxalate in this work's spectra) which induces a different binding energy for the iron 3d orbitals, the similarity is striking and therefore the assignment straightforward. A more detailed discussion is reported in the manuscript.

S3 Experimental parameters

The time-resolved photoelectron spectra were acquired in three different datasets, whose experimental parameters are reported in Table S1.

Each photoelectron spectrum is the average of several acquisitions of 13 seconds each,

for a total acquisition time as reported in Table S1. The experimental uncertainty is computed as standard deviation.

S4 Fit model

The model here described was adopted in this work to describe the kinetics of the PE signal from ferrous species ($I_{Fe^{II}}(t)$), which is proportional to the population kinetics of ferrous species. The population of the ferrous species evolve, upon generation, following a branching. The major fraction $\left(\frac{A_{\infty}}{A_0}\right)$ remains unchanged for the whole investigated time window (250 ps), while a minor fraction $\left(\frac{A_1}{A_0}\right)$ shows exponential decay with time constant τ_1 .

To discern whether there is a prompt or delayed creation of ferrous species after photo-excitation of the aqueous ferrioxalate, the total PE signal amplitude $A_{Fe^{II}}$ is assumed to exponentially rise with time constant τ_R .

The whole intensity is therefore convoluted - \otimes - with the IRF and the LAPE feature summed to the ferrous species PE signal. The analytical equation used to fit the experimental kinetic trace with such a model is the following:

$$I_{Fe^{II}}(t) = \left\{ A_0 \left[1 - e^{-\frac{(t-t_0)}{\tau_R}} \right]_{t>t_0} \left[\frac{A_{\infty}}{A_0} + \frac{A_1}{A_0} e^{-\frac{(t-t_0)}{\tau_1}} \right]_{t>t_0} \right\} \otimes \text{IRF} + \text{LAPE}(t_0, \text{FWHM}) \quad (\text{S1})$$

where A_0 was factorised.

The fit procedure also accounts for the experimental data uncertainty (see error bars in Fig. 4.b and 5) and it propagates it to the fit parameter results. Their values are given with a confidence interval corresponding to 1 standard deviation.

S5 Homogeneous decrease of the transient PES signal in the RoI energy window

In order to discard that the decreasing intensity of the ferrous PE transient signal (Figure 5 in the manuscript) is due to a sliding of the signal towards higher E_B , the tr-LPES 2D map

(here reproduced in Figure S3.a) is analysed in a different fashion. Four integration regions in energy are taken into account within the RoI (5 to 7.5 eV), and the so obtained kinetic traces are displayed in Figure S3.b.

We observe that the shape of the four kinetic traces is the same and the possible spectral intensity energy shift can be discarded. The observed transient signal decay within 5 ps is clearly the same per each slice, *i.e.* the whole band homogeneously decreases in intensity. This supports the interpretation given in the manuscript as due to a decrease of photogenerated ferrous species.

Table S1: Experimental parameters for the tr-PES measurements on ferrioxalate aqueous solution. The 263 nm-wavelength pump beam was focussed on the liquid μ -jet overlapping with the VUV probe beam (focal spot size $\sim 40\mu\text{m}$ FWHM).

parameter	dataset			unit
	1 ps	5 ps	250 ps	
acquisition per time delay	234	350	165	s
solute concentration	0.5	0.5	0.5	Molar
VUV probe	34.0	34.0	37.4	eV
monochromator grating	200	200	200	grooves/mm
pump energy	0.4	0.9	0.28	$\mu\text{J}/\text{pulse}$
pump focal spot (FWHM)	200	200	80	μm
pump fluence	1.4	0.6	2.8	mJ/cm^2
excitation yield	$\sim 3\%$	$\sim 1\%$	$\sim 5\%^1$	-
flow rate	0.3	0.3	0.4	ml/min
jet diameter	~ 17	~ 17	~ 17	μm

¹The calculated excitation yield for the *250 ps dataset* might not correspond to the effective one because the small size of the pump focal spot made the overlap less accurate than for other datasets. Any misalignment implies smaller effective excitation yield.

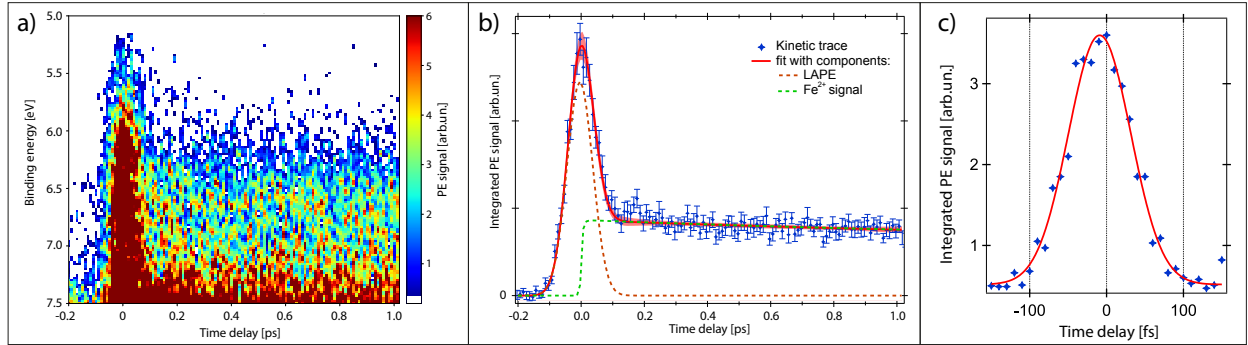


Figure S1: LAPE effect in tr-PES experiments. a) 2D map of ferrioxalate solution in the RoI with predominant LAPE signal around time zero. b) integrated PE signal of a) which displays the signal kinetics and its components: LAPE (orange) and PE signal from ferrous species (green). c) Integrated PE signal on pure-solvent (water): only the LAPE signal is present in the RoI energy range, in red a gaussian fit.

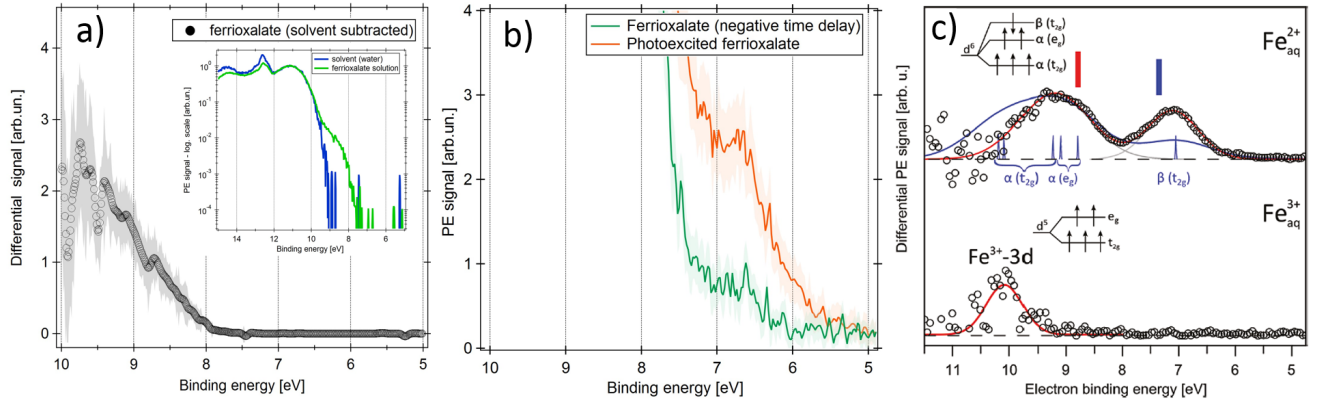


Figure S2: PE spectra of iron compounds in aqueous solution. a) Aqueous ferrioxalate ground state differential spectrum (black); inset: water and aqueous ferrioxalate in logarithmic scale. b) Photoexcited (263 nm - orange) and unexcited (green) aqueous ferrioxalate. c) octahedral hexa-aquated iron compounds in water, with electronic configuration scheme and orbital assignment. Adapted from Seidel *et al.*².

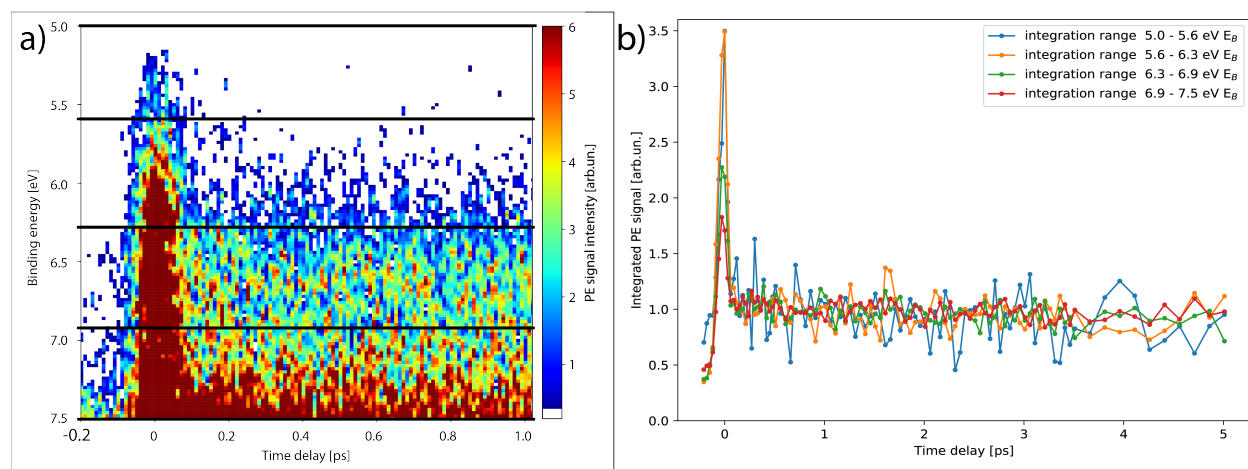


Figure S3: Evidence that the PE signal from ferrous species does not reduce because of a band shift in energy. **a)** 2D map with bold lines which define the integration energy range under scrutiny. **b)** Kinetic traces as the integrated PE intensity in the four energy ranges. There is no evidence of a shift in energy of the PE intensity, which would show a non-homogeneous behaviour of the integrated signal among the energy ranges.

References

- (1) Arrell, C.; Ojeda, J.; Mewes, L.; Grilj, J.; Frassetto, F.; Poletto, L.; van Mourik, F.; Chergui, M. Laser-Assisted Photoelectric Effect from Liquids. *Physical Review Letters* **2016**, *117*, 143001.
- (2) Seidel, R.; Thürmer, S.; Moens, J.; Geerlings, P.; Blumberger, J.; Winter, B. Valence photoemission spectra of aqueous $\text{Fe}^{2+/3+}$ and $[\text{Fe}(\text{CN})_6]^{4-/3-}$ and their interpretation by DFT calculations. *Journal of Physical Chemistry B* **2011**, *115*, 11671–11677.